

THE EFFECT OF ADDING YTTRIUM OXIDE MICROPARTICLES ON THE WEAR RESISTANCE OF ALUMINIUM ALLOY AA5083

ABDULLAH D. ASSI^{1,*}, SALMAN H. OMRAN², AMMAR I. NAJI³,
HUSSAIN A. HUSSAIN⁴, and SARAH A. AL-SHAMMARI⁵

¹Mechanical Engineering Department, College of Engineering,
University of Baghdad, Baghdad, Iraq

²Energy and Renewable Energies Technology Center, University
of Technology- Iraq, Baghdad, Iraq

³Al-Kut Technical Institute, Middle Technical University, Baghdad, Iraq

⁴Advance Welding Solutions Company Ltd. Baghdad, Iraq

⁵Ministry of Sciences and Technology, Baghdad, Iraq

*Corresponding author email: drabdullahdhayea@uobaghdad.edu.iq

Abstract

In this research, aluminium composite matrices based on post-eutectic aluminium alloy were prepared and reinforced with microparticles of yttrium oxide, named Yttria, with weight fractions of 0, 3, 6, and 9 wt.% and with granular size between 40 and 60 μm . The composite materials were prepared by the vortex method, where microparticles have been added to the molten substance, then mixed using a mechanical mixer to create the vortex. Then, microscopic examination, hardness tests and wear rate measurements were performed. The results showed that the presence of Yttria microparticles in different proportions in the microstructure increases the hardness of the aluminium composite alloy compared to the unreinforced alloy. The results also showed better distribution of microparticles. As for the wear rate, it was lower for the composite materials compared to the unreinforced alloy. The wear rate decreased with the increase in weight percentages of microparticles, and the best addition percentage is 9 wt.% Yttria.

Keywords: Aluminium alloy 5083, Composite hardness, Vortex, Wear rate, Yttria, Yttrium oxide.

1. Introduction

Composite matrix based on aluminium alloys is used in applications that require good mechanical properties with light weight. The application of these materials is based on improving the mechanical properties at high temperatures and wear resistance compared to non-reinforced alloys. Important applications in which these materials are used are aerospace and vehicles, shipbuilding, ship hulls, observation masts and other marine structures, the automobile industry, aircraft and helicopter manufacturing, petroleum and chemical industries such as building piping systems and equipment for the oil and gas industry and chemical industries due to their resistance to corrosion in harsh environments, as well as military applications where they are used. This alloy is used in the manufacture of vehicles and military equipment because of its durability and strength [1, 2].

An important alloy in industrial applications is AA5083 because of its properties such as low density, high thermal conductivity, high strength, and high wear resistance [3, 4]. Aluminium Metal Matrix Composites (ALMMCs) are widely manufactured in a solid state as powder metallurgy or liquid state as a stir casting technique [5, 6]. The stir casting process is the preferred technique because it is easy, simple and can be used for a wide range of materials [7]. Several ceramics materials such as SiC, SiO₂, Al₂O₃, TiO₂, B₄C, and carbon are used as reinforcements of AA 5083 to produce composite materials with desirable properties [8, 9]. Bates et al. [10] studied the effect of silicon carbide on the mechanical properties of AA6061 fabricated by stir casting technique. The effect of silicon carbide on the mechanical properties of AA6061 manufactured by stir casting technique was studied. Silicon carbide was added at different weight concentrations. The results of this work showed that it improved the tensile strength, impact strength, hardness, and wear resistance [11, 12].

The resistance to friction and wear are some of the most important properties that require improvement because of their importance in many applications, such as engine pistons and bearings [13]. Although aluminium alloys have what qualifies them for use in such applications, they do not have the required resistance under conditions of dry friction [14]. Therefore, researchers studied them and identified the possibilities through which the property of resisting friction and wear can be improved [15, 16]. One of the methods that improve this property is the addition of ceramic materials [17]. There is much research that has addressed the addition of various ceramic particles [18, 19]. However, there is little research related to the addition of Yttria (Y₂O₃), especially for aluminium alloy (AA5083). After the impact and wear characteristic, this is what we will try to study in this research.

The research problem is that the properties of aluminium alloys suffer relatively low hardness and high wear rate to be used in a certain industry, like space structures and military equipment. Enforcement of aluminium alloys by yttrium oxide particles, in particular, AA5083 alloy could provide better hardness and less wear rate.

This research aims to study the wear and hardness properties of a matrix consisting of AA5083 alloy and reinforced with microparticles of Yttria, known as Yttria, with different weight fractions 0, 3, 6, and 9 wt.% of Yttria and with a granular size between 40 - 60 µm by vortex method. The experiments have been performed at various sliding times (t) of 5, 10, and 15 min and applied loads 10 and 20 N.

2. Experimental Work

2.1. Metal matrix

The chemical basis describes the extent to which the electric field affects the behaviour of fire within the combustion process due to the presence of ionic species. Much literature has dealt with the effect of the electric field on the flame to improve the flame properties, starting with flame speed and stability, flame front brightness and flame composition, and pollutant emissions [18, 20]. Moreover, it verified the possibility of electric fields being considered one of the flame control triggers. As a result of the electron transfer or ionisation accompanying the collision process or chemical ionisation, ions are formed in the flame. Singh et al. [21] demonstrated that the reaction in the hydrocarbon combustion process was a reason to produce H_3O^+ ion, while the reaction produces CHO^+ ion:

The base alloy, aluminium 5083, was used. Table 1 shows the chemical composition of this alloy and Table 2. Mechanical and physical properties of AA5083. Chemical analysis and properties of the alloy were conducted using an atomic absorption device at the Ministry of Science and Technology (AA-6800 Shimadzu, Japan).

Table 1. Chemical composition of aluminium alloy AA5083.

Element wt.%	Mn	Cu	SiC	Zn	Ti	Cr	Mg	Fe	Al
Standard [22]	4-4.9	0.4-1	0.4	0.25	0.05-0.25	0.05-0.25	0.15	0.1	92.7
Measured	4.5	0.66	0.3	0.23	0.2	0.19	0.12	0.1	93.7

Table 2. Mechanical and physical properties of AA5083.

Material AA5083	Density (gm/cm ³)	VHN (kg/mm ²)	UTS (MPa)	YS (MPa)	Elongation (%)	E (GPa)
Standard [22]	2.66	87	290	145	12-27	71
Measured	2.6	85	285	140	15	70

2.2. Vortex method

Yttria fines were used in powder form with a granular size between 40-60 μm , which was measured through an England Ridsdale & Co LTD vibrating screening device for 10 minutes. The composite matrix was prepared by melting pieces of the base alloy AA5083 with a weight of 194 gm Inside an alumina shell in an electric furnace (Townson, England) at a temperature of 700°C. After that, the shell containing the molten was transferred and then placed in a cylindrical open-mouth electric furnace at a temperature of 750°C. Yttria Chips weighing 6 gm were then added after being wrapped in pure aluminium foil to obtain a percentage of 3%. It was heated, and then the mechanical mixing process was carried out for 5 minutes to create the vortex. The system used to create the vortex consists of an Electric mixer equipped with a steel fan that rotates at a rotational speed of 300 rpm. After the vortex and mixing of the melt, the melt was poured into a pre-dried steel mould, and the casting was left to solidify in still air. Similarly, all samples were prepared with varying weight fractions of Y_2O_3 microparticles to investigate their influence on the composite properties [8, 23].

2.3. Microstructure examination

Samples of the prepared alloy (AA5083) reinforced with Ytria microparticles were taken and smoothed with paper with different degrees of silicon carbide distribution 320, 500, 1000 and 1200 using a device (Struers DAP-5, Denmark). The samples were then polished using alumina powder with a granular size of 0.3 mm. After that, the samples were removed using 0.5% HF], washed with water, then alcohol, and then dried with hot air. The microstructure was then examined by an optical microscope (100 W Carlzeiss Jane, Germany) with a digital camera of 5 Megapixels.

2.4. Hardness test

The hardness test was conducted using the Vickers Hardness method by a device (Zwick & Co., Germany). The hardness number was calculated by taking the average of three readings for each sample and using a load of 500 g. The test has been performed according to ASTM standards [22, 24].

2.5. Wear rate test

The wear test was used in a pin-on-disk wear test device under dry conditions after preparing its samples in the same way as preparing samples for microscopic examination, but without showing. The samples were of a diameter of 1 cm and a length of 2 cm. The values of the variables that were adopted in these tests are:

- i. Sliding time (t): 5, 10, 15 min
- ii. Applied load: 10, 20 N

The wear rate was calculated through the following relationship [25]:

$$W_r = \frac{\Delta w}{2\pi} \cdot r \cdot N \cdot \rho \cdot t \quad (1)$$

where W_r is the wear rate (cm^3/cm), Δw is the difference in weight before and after the test (gm), and r is the distance from the centre of the sample to the centre of the sliding disc, which is 7 cm. N is the number of revolutions per minute of the steel disc, which is set to 550 rpm, and ρ is Sample density (gm/cm^3).

A carbon steel disc with a hardness of (35HRC) was used to test the wear. The test samples were installed in the holder, and a balancing operation was carried out for the arm carrying the sample holder (Specimen Holder).

Before conducting the test for each sample, contact between the sample surface and the facing steel disc was ensured. After each test, the disc—specifically the contact area—was smoothed using grade (500, 1000) smoothing papers to maintain a consistent level of initial surface roughness and to remove any material transferred from the test sample.

For samples, the wear rates for the samples were calculated by measuring the weight of each sample before starting the test and then measuring the weight of the sample after completing the test using a sensitive type of balance Mettler AE200 Switzerland with an accuracy of ± 0.0001 g. ASTM standard was followed to perform the prediction of the wear rate [22, 25].

3. Results and Discussion

3.1. Microstructure

Figure 1(a) shows the microstructure of the post-eutectic aluminium alloy AA5083. The figure shows the microstructure consisting of eutectic with a primary aluminium phase and a small number of primary elements. The reason for the alloy contains a number of added elements, such as copper, in addition to a number of impurities. These elements can increase the cooling rate of the alloy when it is poured into metal moulds after mechanical stirring. When the cooling rate is increased, the eutectic point tends towards the element with the lower percentage, and thus, the primary aluminium phase is formed when the alloy is poured [26].

Figures 1(b), 1(c), and 1(d) show the microstructure of the composite materials consisting of the base alloy and Yttria microparticles, AA5083- Y_2O_3 , with addition rates of 0, 3, 6, and 9 wt.%, respectively. The results of the microscopic examination shown in these figures showed the presence of Yttria microparticles in the base alloy. The presence of microparticles also increases with the addition rate and mixing speed, as the mixing speed used was high, which leads to the distribution of the particles in the parts of the mould. Also, the distribution increases with increasing the percentage of microparticles added. There are also some agglomerations of the added microparticles. The best distribution occurred at the addition rate of Yttria microparticles, which was 9wt.%. Through these microscopic shapes, it was observed that there is an amount of Yttria microparticles added to the outer circumference of the casting. The reason is due to the high mixing speed used, which leads to an increase in the centrifugal force of the liquid and makes the microparticles move towards the sides of the casting and may be the reason for its agglomeration as well [27].

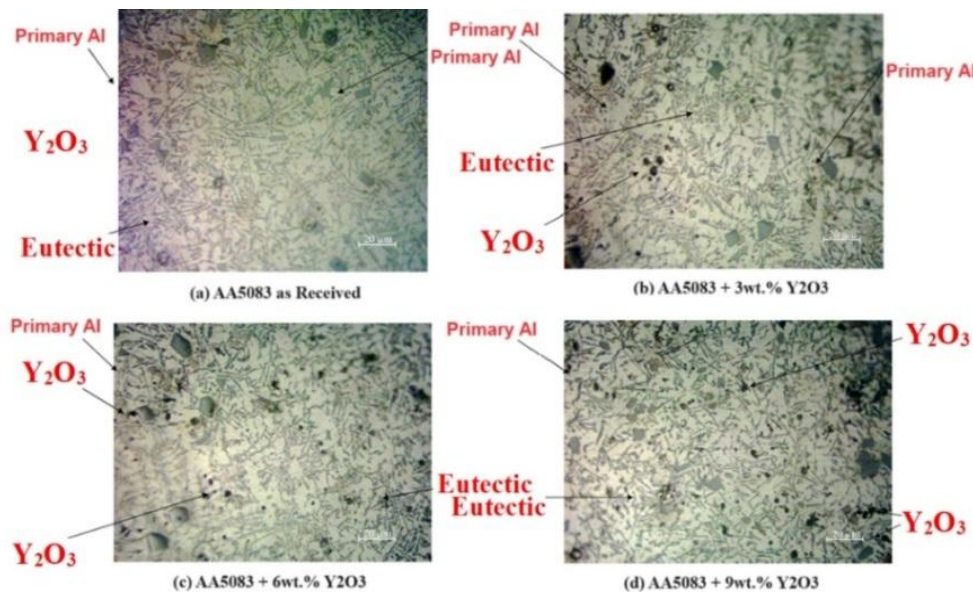


Fig. 1. Microstructure of the composite matrix AA5083 + 0, 3, 6, 9 wt.% of Yttria.

3.2. Hardness

Figure 2 shows the relationship between the hardness and the weight percentages of the added Yttria microparticles. It is observed from the figure that the hardness of the composite materials is greater than the hardness of the base alloy due to the action of the microparticles in addition. The hardness also increases with the increase in weight percentages of the microparticles because the hardness of the microparticles themselves is high. The highest percentage of hardness was when 9 wt.% of Yttria microparticles were added [28].

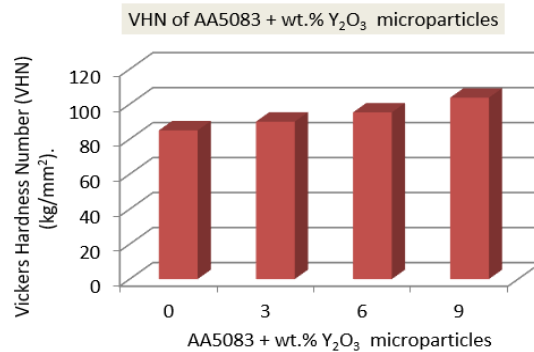


Fig. 2. Hardness relationship with weight percentages of Yttria microparticles in the composite matrix.

3.3. Wear rate

Figure 3 shows the relationship between the wear rate and the weight percentage of the Yttria microparticles at a sliding time of 5 minutes, in which it was observed that the wear rate for all the composite materials is less than the wear rate of the base alloy. Also, the wear rate decreases with the increase in the percentage of microparticles, and this is due to the increase in hardness with increasing Yttria microparticles, as stated in the hardness results. When the sliding time was increased to 10 minutes, it was observed that the wear rate decreased with the increase in the percentage of microparticles, and the wear rates increased with the further increase in the sliding time to 15 minutes [29].

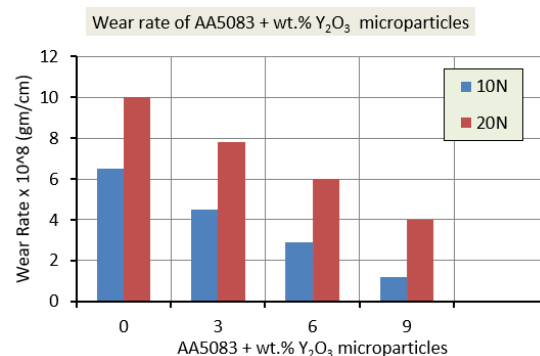


Fig. 3. The relationship of the wear rate with the weight percentages of the composite matrix at a time of 5 minutes.

Figure 4 shows the relationship between wear rate and sliding time for AA5083 alloy with constant applied load. It was observed that the wear rate increased with increasing sliding time. The same situation exists in the composite materials shown in Figs. 5-7. The increase in the wear rate is due to the separation of some microparticles from the sample, and these separated minutes are called (debris) and act as a solid part that increases the wear of the sample. The reason for the slight decrease in the wear rate in Fig. 5. at a sliding time of 10 minutes may be due to the occurrence of errors in conducting the wear test in terms of stabilising the test sample.

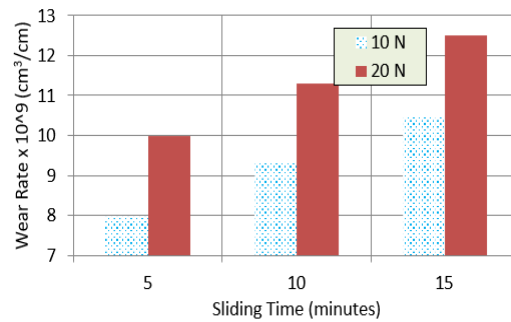


Fig. 4. Wear rate at various sliding times for the base alloy AA5083 at 10 and 20 N loads.

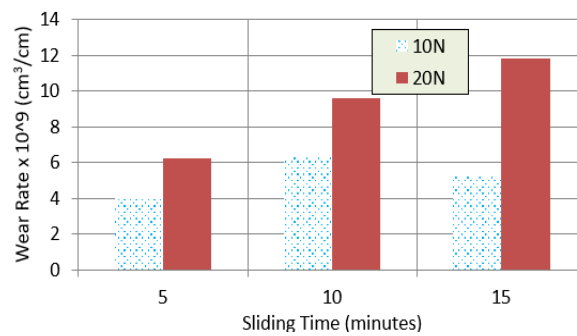


Fig. 5. Wear rate at various sliding times for the composite matrix AA5083 + 3 wt.% Y₂O₃ at 10 and 20 N loads.

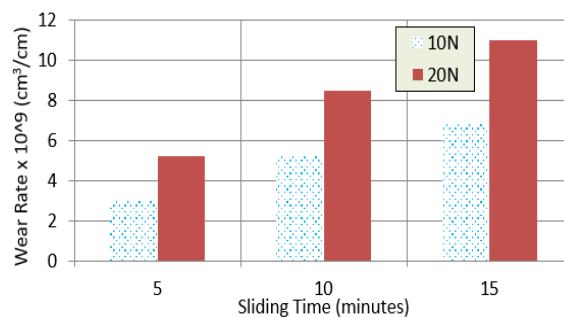


Fig. 6. Wear rate at various sliding times for composite matrix AA5083 + 6 wt.% Y₂O₃ at 10 and 20 N loads.

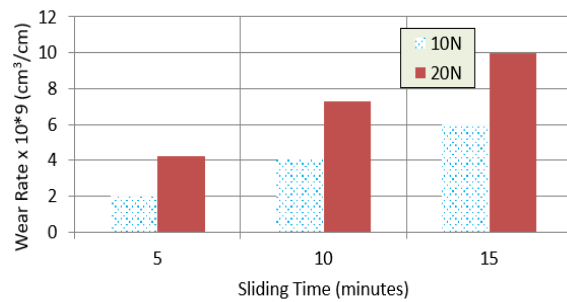


Fig. 7. Wear rate at various sliding times for composite matrix AA5083 + 9 wt.% Y_2O_3 at 10 and 20 N loads.

Figure 8 shows the relationship between wear rate and applied load for AA5083 alloy with constant sliding time. The increase in the wear rate with the increase in the applied load is due to the increase in the number of small particles (debris) separated from the sample material (the overlapping material) because of the increase in friction and pressure with the hard disc of the device. These particles increase the wear on the surface of the sample because they act as concentrated stress on the sample in the areas where they are located. The same situation exists in Figs. 9-11, which is an increase in the wear rate with an increase in the applied load and for all the overlapping materials, as well as a transition in the type of wear from (light wear to severe metallic wear) at different times and high loads.

The metal wear mechanism occurs because the loading pressure can completely break down the oxides formed on the surface subjected to wear. As a result, a metal contact will occur, which leads to a complete coalescence between the two surfaces. The breaking of this coalescence because of continued sliding leads to the formation of wear particles. The mineral (debris) mentioned above separates from the superimposed matter. As the applied load increases, these metal particles (debris) increase through the separation mechanism and act as additional centres to increase wear and may cause plastic distortion on the surface of the sample and deep cracks due to friction. Through all the previous figures, it was observed that the lowest wear rate was at the highest weight percentages of Yttria microparticles due to their high hardness. Also, the lowest wear rate was at the lowest sliding time and the lowest applied load.

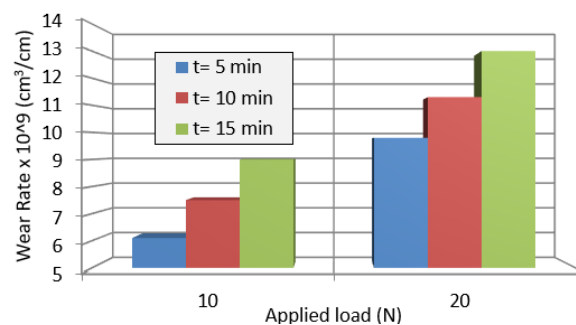


Fig. 8. The wear rate with the applied load of the base alloy AA5083 at different times.

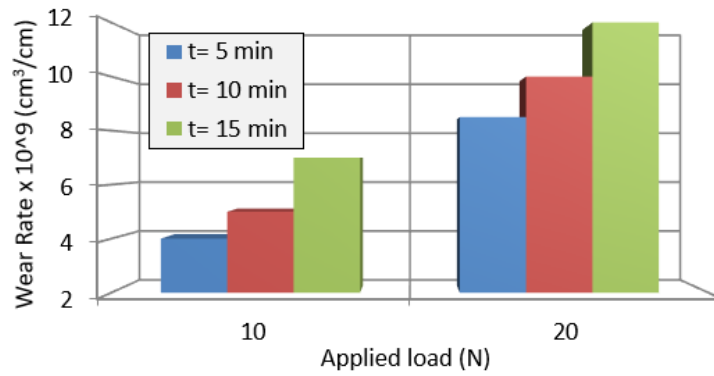


Fig. 9. The wear rate with the applied load of the composite matrix AA5083 + 3 wt.% Y_2O_3 at various times.

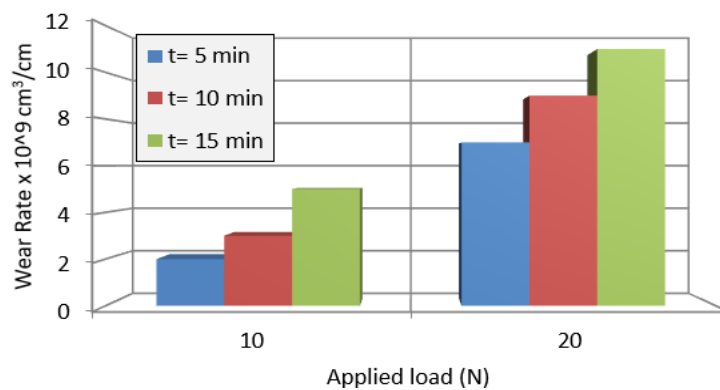


Fig. 10. The wear rate with the applied load of the composite matrix AA5083 + 6 wt.% Y_2O_3 at various times.

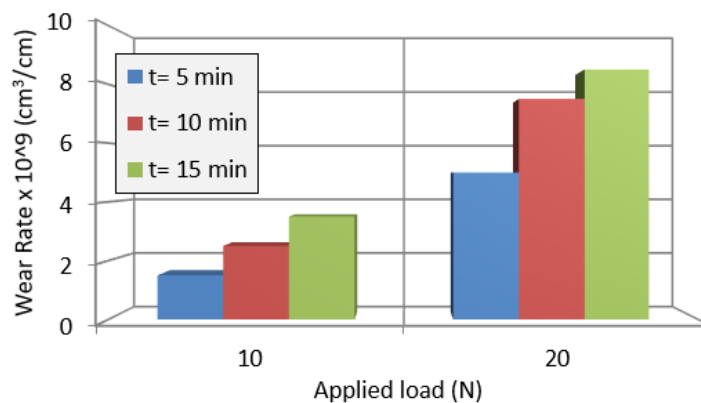


Fig. 11. The wear rate with the applied load of the composite matrix AA5083 + 9 wt.% Y_2O_3 at various times.

4. Conclusions

The composite matrix was prepared by the vortex method, where the particles were added to the molten substance and then mixed with a mechanical mixer to create the vortex; then the material was poured into cylindrical metal moulds and microscopic examination and hardness tests were conducted using the Vickers method and wear rate. The results showed better distribution of the particles and higher hardness with an increase in the volume fraction of Ytria microparticles [30]. The following conclusions were obtained:

- The wear rate decreases with increasing weight percentages of Ytria microparticles added to the base alloy AA5083 and all percentages.
- The transition from light wear to severe wear depends on the material used and is slight at short sliding times and large and clear at high times and heavy loads, which act as additional centres of wear on the surface of the sample.
- The best hardness and lowest wear rate are at the highest weight percentage used, which is (AA5083-9 wt.% Y₂O₃).

Nomenclatures

T	Temperature, °C, K
t	Time, Sec
HV	Vickers Hardness
W_r	Wear Rate, cm ³ /cm
wt. %	Weight percentage

Greek Symbols

ρ	Sample density, kg/m ³
--------	-----------------------------------

Abbreviations

ALMMCs	Aluminium Metal Matrix Composites
AA5083A508	Aluminium Alloy 5083
Y ₂ O ₃	Yttrium oxide

References

1. Parikh, V.K.; Patel, V.; Pandya, D.P.; and Andersson, J. (2023). Current status on manufacturing routes to produce metal matrix composites: State-of-the-art. *Heliyon*, 9(2), e13558.
2. Golla, C.B.; Pasha, M.B.; Rao, R.N.; Ismail, S. and Gupta, M. (2023). Influence of TiC particles on mechanical and tribological characteristics of advanced aluminium matrix composites fabricated through ultrasonic-assisted stir casting. *Crystals*, 13(9), 1360.
3. Hassin, M.J.; and Salman, T.A. (2023). Corrosion inhibition efficiency investigation of yttrium oxide nanoparticles coated on carbon steel alloy. *Baghdad Science Journal*, 20(6).
4. Omran, S. H.; Assi, A.D.; Ali, M.H.; Shandook, A.A.; Abbud, L.H.; and Abdul Wahhab, H.A. (2023). Fatigue and hardness behavior of AL-2CU-2MG alloy due to titanium dioxide and silicon carbide nanoadditives. *Journal of Engineering Science and Technology (JESTEC), Special Issue*, 18(6), 240-254.

5. Guerrero, C.T. et al. (2022). An overview of the interactions between reinforcements and Al matrices with Si, Cu and Mg as alloying elements in aluminium matrix composites: Case of Oxide Reinforcements. *Materials Research*, 25, e20210540
6. Sankhla, A.M. et al. (2022). Effect of mixing method and particle size on hardness and compressive strength of aluminium based metal matrix composite prepared through powder metallurgy route. *Journal of Materials Research and Technology*, 18, 282-292.
7. Kumar, B.R.S. et al. (2022). Investigations on wear behavior of aluminium composites at elevated temperature. *Advances in Materials Science and Engineering*, 2022(1), 9594798.
8. Assi, A.D. (2020). Influence of Al₂O₃ Nanoparticles Addition to AA6082-T6 on Mechanical Properties by Stir Casting Technique. IOP Conference Series: *Materials Science and Engineering*, 881(1), 012081.
9. Parikh, V.K.; Badgujar, A.D.; and Ghetiya, N.D. (2022). Effect of friction stir processing parameters on microstructure and microhardness of aluminium based metal matrix composites. *Materials Today Proceedings*, 62(14), 7455-7460.
10. Bates, W.P. et al. (2023). Properties augmentation of cast hypereutectic Al–Si alloy through friction stir processing. *Metals and Materials International*, 29, 215-228.
11. Assi, A.D.; Abdulhadi, H.A.; and Omran, S.H. (2020). Effect of adding SiC and TiO₂ nanoparticles to AA6061 by stir casting technique on the mechanical properties of composites. *Journal of Mechanical Engineering Research and Developments*, 43(6), 167-183.
12. Chitra, R.; Jegan, T.M.C.; Bamini, A.M.A.; Glivin, G. and Frankin, V.A. (2023). *Stir casting process parameters and their influence on the production of AA6061/B4C metal matrix composites*. In Chitra, R.; Jegan, T.M.C.; Bamini, A.M.A.; Glivin, G. and Frankin, V.A. (Eds.), *Advances in Processing of Lightweight Metal Alloys and Composites*. Springer, Singapore.
13. Woźnicki, A. et al. (2021). Homogenisation of 7075 and 7049 aluminium alloys intended for extrusion welding. *Metals*, 11(2), 338.
14. Parikh, V.K.; Badheka, V.J.; Badgujar, A.D.; and Ghetiya, N.D. (2021). Fabrication and processing of aluminium alloy metal matrix composites. *Materials and Manufacturing Processes*, 36(14), 1604-1617.
15. Karthik, R.; Gopalakrishnan, K.; Venkatesh, R.; Krishnan, A.M. and Marimuthu, S. (2022). Influence of stir casting parameters in mechanical strength analysis of aluminium metal matrix composites (AMMCs). *Materials Today Proceedings*, 62(4), 1965-1968.
16. Alalkawi, H.J.M.; Khenyab, A.Y.; and Ali, A.H. (2019). Improvement of mechanical and fatigue properties for aluminium alloy 7049 by using nano composites technique. *Al-Khwarizmi Engineering Journal*, 15(1), 1-9.
17. Keshavara, H.; Kokabi, A.; and Movahedi, M. (2023). Microstructure and mechanical properties of Al/graphite- zirconium oxide hybrid composite fabricated by friction stir processing. *Materials Science and Engineering: A*, 862, 144470.
18. Salman, K.D. (2019). Abrasive wear characteristics of composite material (AA 7075 / SiC) synthesised by stir casting. *Journal of Engineering*, 25(1), 32-39.

19. Yang, H. et al. (2022). Effect of different sintering additives on microstructure, phase compositions and mechanical properties of Si₃N₄/SiC ceramics. *ES Materials & Manufacturing*, 15(4), 65-71.
20. Mehdi, H.; and Mishra, R.S. (2021). Effect of multi-pass friction stir processing and SiC nanoparticles on microstructure and mechanical properties of AA6082-T6. *Advances in Industrial and Manufacturing Engineering*, 3, 100062.
21. Singh, N.; Belokar, R.M.; and Walia, R.S. (2021). Experimental investigation on microstructural and mechanical attributes of Al 7075-T6/SiC/CR/MoS₂ based green hybrid composite via advanced vacuum-sealed bottom pouring stir casting. *Silicon*, 14, 7643-7665.
22. Glazman, J.S.; and Rumble, J.R. (1989). *Computerisation and Networking of Materials Data Bases*. ASTM International.
23. Wang, Y. et al. (2022). Enhanced mechanical properties of in situ synthesised TiC/Ti composites by pulsed laser directed energy deposition. *Materials Science and Engineering: A*, 855, 143935.
24. Zhang, X. et al. (2022). Microstructure and enhanced mechanical properties of ZrC/Zr composites added by in-situ Y₂O₃ reinforced particles. *Vacuum*, 203, 111277.
25. Mercado-Lemus, V.H. et al. (2021). Wear dry behaviour of the Al-6061-Al₂O₃ composite synthesised by mechanical alloying. *Metals*, 11(10), 1652.
26. Alagarsamy, S.V.; Ravichandran, M.; and Meignanamoorthy, M. (2022). Multi-objective optimisation of dry sliding wear control parameters for stir casted AA7075- TiO₂ composites using Taguchi-Grey relational approach. *Australian Journal of Mechanical Engineering*, 20(5), 1453-1462.
27. Oguntuyi, S.D.; Shongwe, M.B.; Tshabalala, L.; Johnson, O.T.; and Malatji, N. (2022). Effects of SiC on the microstructure, densification, hardness and wear performance of TiB₂ ceramic matrix composite consolidated via spark plasma sintering. *Arabian Journal for Science Engineering*, 48, 2889-2903.
28. Wang, L. et al. (2021). Lightweight Zr_{1.2}V_{0.8}NbTi_xAl_y high-entropy alloys with high tensile strength and ductility. *Materials Science and Engineering: A*, 814, 141234.
29. Mythreyi, O.V.; Nagesha, B.K.; and Jayaganthan, R. (2022). Microstructural evolution & corrosion behavior of Laser –powder-bed–fused Inconel 718 subjected to surface and heat treatments. *Journal of Materials Research and Technology*, 19, 3201-3215.
30. Kök, M.; and Özdin, K. (2007). Wear resistance of aluminium alloy and its composites reinforced by Al₂O₃ particle. *Journal of Materials Processing Technology*, 183, 301-309.